5G Sub-6 GHz Wideband Antenna with PSO Optimized Dimensions

Heba Y. M. Soliman[1, *], Amany A. Megahed[2],
Mohamed Abdelazim[3], and Ehab H. Abdelhay[4, 5]

Abstract—In this paper, a rectangular patch antenna that covers the band from 3.2 to 5.7 GHz to support 5G New Radio (NR) sub-6 GHz with high gain and efficiency is designed and implemented. Particle Swarm Optimization (PSO) algorithm is used to get the dimensions of the antenna and slots. The optimization goals are to reach the smallest dimensions of the antenna in the required bandwidth keeping scattering parameter at port 1 $|S_{11}|$ below -10 dB, a gain of 4 dBi or higher, and efficiency more than 90%, respectively. The resonance frequency of a microstrip patch is 4.45 GHz. PSO using the computer simulation tool (CST) software is used to design an antenna with desired frequency response and radiation characteristics for 5G New Radio (NR) sub-6 GHz. The antenna is designed over an FR-4 substrate with a noticeable reduction in cost, simplicity in design, and a small overall size of $23 \times 15 \, \text{mm}^2$. The antenna is with the partial ground. The antenna has two parallel stubs and EL slots; the lengths of these slots control the desired bandwidth. A high agreement between the simulated and measured results is noticed.

1. INTRODUCTION

The huge growth in mobile services' subscribers around the world makes companies and research teams pay attention to mobile base station costs and improve their electrical features such as bandwidth and efficiency. Advanced radiation properties, reduction in size, and high efficiency are the main important considerations for antenna design required to occupy a smaller possible space. Accordingly, current literature is working on the improvement of cost-effective, lightweight, small size, and low-profile antennas with the capability of wideband coverage with high efficiency [1–7]. Many optimization techniques such as Genetic Algorithm (GA), Artificial Neural Network (ANN), and Particle Swarm Optimization (PSO) are introduced in science, engineering applications, and communication systems such as in [8]. Optimization techniques are used in antenna design to select the best element design and dimensions regarding some criteria from a certain set of available alternatives. PSO was used in many research efforts to develop a microstrip antenna [9–11]. For example, in [12], recent developments in using PSO to improve side-lobe level and beamwidth in uniform and nonuniform antenna arrays for antenna design applications are presented. In [13], the PSO of Log-Periodic Dipole Arrays (PDAs) is used to show the performance of several radiation parameters. Several works employed PSO to solve different electromagnetics problems such as the optimization of the Yagi-Uda antenna [14, 15]. An improved PSO algorithm is introduced, in which the parameter inertia weight is dynamically controlled through PSO optimization combined with Finite Difference Time Domain (FDTD) to design a broadband microstrip patch antenna. In [16], a neural network is used for synthesizing an antenna array with 10 equally spaced elements with Side Lobe Level (SLL) approaching -20 dB and getting the amplitude of each element. In [17], a four-port MIMO array with high isolation between ports is proposed. The proposed antenna

array has the dimensions of $46\,\text{mm} \times 46\,\text{mm} \times 1.6\,\text{mm}$ using an FR-4 substrate. In [18], the authors introduce a single polarization antenna with an RO4350B substrate ($\varepsilon_r = 3.48$ and $0.76\,\text{mm}$ thickness) that covers the band from 1.54 to 2.86 GHz. In [19], an orthogonal printed dipole with an adjusted integrated balun to cover the band from 1.6 to 2.7 GHz is designed. It is fabricated on FR4 material with a dielectric constant of 4.3, a total size of $1100 \times 150\,\text{mm}^2$, and a thickness of $1.5\,\text{mm}$. In [20], the authors use discrete PSO (DPSO) for return loss improvement and optimization of microstrip antenna using GA for patch miniaturization. [21] introduces a square patch microstrip antenna suitable for the frequency of 2.45 GHz. [22] presents a dual-polarized multilayer antenna on an FR4 substrate with a band ranging from 1.83 to 2.2 GHz, while Elsherbini et al. [23] introduce a dual-polarized antenna on a RO4300C substrate — increasing the cost of the antenna — to cover the band from 1.71 to 2.17 GHz with a noticeable size reduction compared to [22]. In [24], PSO is used to design and optimize the proposed patch antenna using High Frequency Structure Simulator (HFSS). The antenna gain is set to 4.5 dBi at 5.2 GHz. In [25], PSO is selected to design an antenna for WLAN/WIMAX with a gain of 3.4 dBi [26]. An antenna is designed to cover the band from 3.2 to 5.7 GHz, but the gain and efficiency of the antenna are 2.2 dBi and 75%, respectively. In this paper, the PSO is performed to optimize the dimensions of the microstrip antenna with partial ground to support 5G New Radio (NR) sub-6 GHz n77/n78/n79 and 5 GHz WLAN, in which the n77 (3.3 to 4.2 GHz), n78 (3.3 to 3.80 GHz), and n79 (4.4 to 5.0 GHz) require a wideband coverage of at least 3.3 GHz to 5.0 GHz. The antenna covers the high-frequency range extending from 3.2 to 5.7 GHz. It is fabricated on an FR4 substrate with a dielectric constant of 4.3 which reduces the cost of the antenna with simplicity in structure. After getting the dimensions of the antenna from the PSO algorithm, the antenna is designed using Computer Simulation Technology (CST) to ensure the results. The optimization goals are to reach the smallest dimensions of the antenna in the required bandwidth keeping $|S_{11}|$ below $-10\,\text{dB}$, a gain of $4\,\text{dBi}$ or higher, and efficiency more than 90%, respectively. Excellent agreement is obtained between the simulated and experimental results. The best size achieved is $(19.6 \times 12)\,\text{mm}^2$ with a thickness of $1.6\,\text{mm}$.

This paper is organized as follows. Section 2 explains PSO algorithm. Section 3 describes the antenna design and configuration. Section 4 shows the results and discussions. Finally, the conclusion is shown in Section 5.

2. PARTICLE SWARM OPTIMIZATION

Many optimization approaches such as Genetic Algorithm (GA), Artificial Neural Network (ANN), and Particle Swarm Optimization (PSO) are used in research, engineering, and communication systems. Kennedy and Eberhart [27] were the first to introduce PSO in 1995. Because of its simple implementation and fewer regulating factors, the PSO algorithm has gained a lot of attention from researchers in the recent decade. PSO is a computer method for solving problems by iteratively trying to enhance a candidate solution in terms of a quality metric. In terms of convergence, PSO is faster than GA [28–30]. PSO optimization is preferred because it is simple to construct and just takes a few parameters, and the operator does not evolve or mutate, making it more efficient in some circumstances. The PSO is one of the population-based stochastic optimization techniques. The PSO algorithm is superior in terms of complexity, accuracy, iteration, and program simplicity in finding the target. For its search space, PSO is more flexible in maintaining a balance between global and local searches. Because of the advantages of PSO, PSO becomes a promising candidate for optimizing a wide variety of real-world optimization problems and applications. In [31], a comprehensive survey on PSO with the benefits and drawbacks compared to some optimization algorithms is presented. In [32], PSO is used to optimize the phase distribution on the transmit array to decrease the side-lobe level of the antenna to operate at 28 GHz. In [33], PSO is used to synthesize the pattern of the antenna.

Each individual in PSO is treated as a "particle" with no volume or mass, which offers a possible solution to a problem. These particles move at a constant speed through the search space. Their velocities are dynamically modified based on information about each particle's past best performance and its neighbors' best previous performances. The particles are expected to flow towards better solution locations. Random initialization m-particles form a community in a D-dimensional target search space, and it is assumed that the ith particle's space position is $X_i = (x_{i1}, x_{i2}, x_{i3}, \ldots, x_{iD})$, $i = 1, 2, \ldots, m$. Each particle has a fitness value determined by its position vector, and to evaluate the

particle X_i, the PSO algorithm finds the optimal solution by iteration. The velocity of each particle in the search space is $V_i = (v_{i1}, v_{i2}, v_{i3}, \ldots, v_{iD})$. The best position of the ith particle is described as $P_i = (P_{il}, P_{i2}, P_{i3}, \ldots, P_{iD})$, and the best fitness value is the appropriate fitness value F_i. The best position of all the particles is considered as the global best position $P_g = (p_{gl}, P_{g2}, P_{g3}, \ldots, P_{gD})$, and the associated fitness value is the global best fitness value F_g. The algorithm adapted uses a set of particles flying over a search space to locate a global optimum. During PSO iteration, each particle updates its position based on its previous position and its neighbors' positions.

$$v_{id} = wv_{id} + c_1 r_1 (P_{id} - X_{id}) + c_2 r_2 (p_{gd} - X_{id}) \tag{1}$$
$$x_{id} = x_{id} + v_{id} \tag{2}$$

where w is the inertia weight; the acceleration coefficients c_1 and c_2 are two positive constants; r_1 and r_2 are two random variables in the range $[0, 1]$. The particle's new velocity is calculated using Eq. (1) based on its previous velocity, its best position, and the group's best experience. In Eq. (1), the first part is caused by the previous speed, called the "inertia" part, which represents the self-confidence motion of the particle in the current state; the second part is the "cognition" part, which represents the private thinking of the particle itself, which is the influence of the previous particle itself best information to the next behavior; the third part is the "social" part, which shows the information sharing and cooperation between particles, and the influence of group best information on the behavior of particles next step. The position adjustment caused by particle interaction is represented by Eq. (2). The procedure of the PSO algorithm is stated in the flow chart shown in Fig. 1. The fitness function $|S_{11}|$ has to be less than -10 dB in the desired band as shown in Eq. (3). In our design, the inertia weight is 1. c_1 and c_2 are equal to 2. The maximum number of iterations is 15, and the maximum number of solver evaluations is 451 for the swarm size. The equation of optimization is

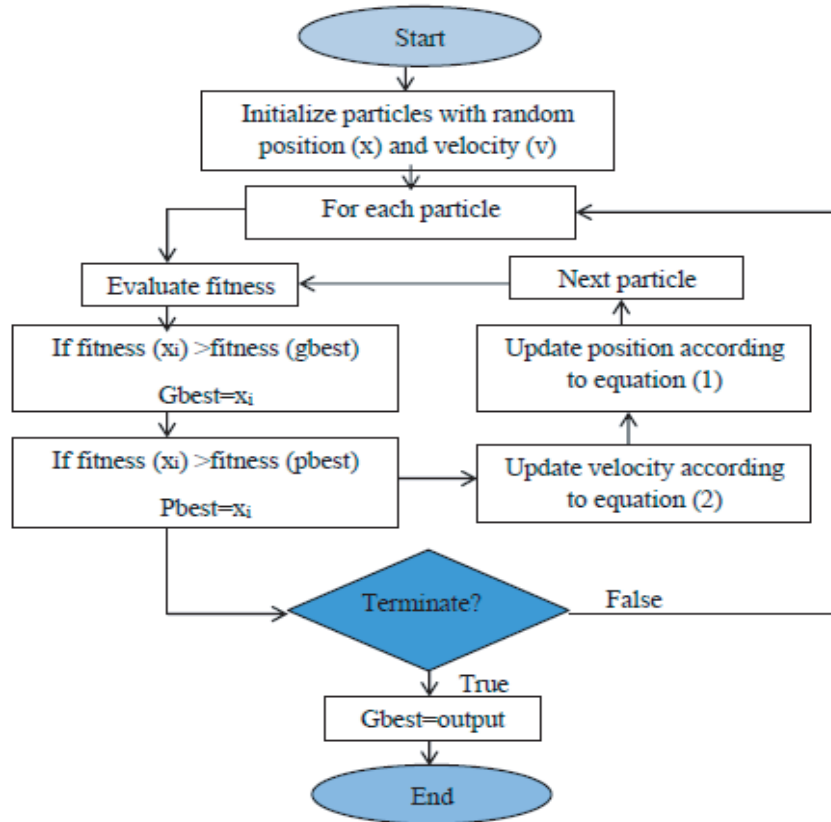$$S_{11}(f) = -20 * \log|\Gamma|, \quad |\Gamma| <= 1, \tag{3}$$

Figure 1. PSO algorithm schema.

$\Gamma = \frac{Z_{in} - Z_o}{Z_{in} + Z_o}$, where f is the frequency that is $f \in (3, 5.7)$ GHz, Γ the antenna's reflection coefficient, Z_o the coaxial feed's characteristics input impedance of antenna $= 50\,\Omega$ for matching, and Z_{in} the antenna's input impedance indicated in Eq. (11).

3. ANTENNA DESIGN AND CONFIGURATION

Figure 2 illustrates the proposed antenna using a CST simulator and fabricated on a substrate of FR4 material with a dielectric constant ε_r of 4.3 and a loss tangent of 0.002. The substrate has a thickness of 1.6 mm. EL slot and two stubs, which are printed on the front side, are inserted on the microstrip rectangular patch antenna to increase the bandwidth. By the use of these two stubs that couple with the partial ground, additional capacitive reactance is mitigated which improves the bandwidth of the antenna. The dimensions of the antenna are determined by Equations (4), (5), and (6) and are used as initial dimensions for the PSO algorithm.

$$W_p = \frac{c}{4f_o\sqrt{\frac{\varepsilon_r + 1}{2}}} \tag{4}$$

$$L_{patch} = \frac{c}{4f_o\sqrt{\varepsilon_{eff}}} \tag{5}$$

$$\varepsilon_{eff} = \frac{\varepsilon_r + 1}{2} + \frac{\varepsilon_r - 1}{2}\frac{1}{\sqrt{1 + 12\frac{h}{w_p}}} \tag{6}$$

where L_{patch} ranges from 10 to 14 mm; W_p ranges from 10 to 13.5 mm; L_{stub} ranges from 5.4 to 6.6 mm; L_{feed} ranges from 6 to 8 mm; W_L ranges from 0.9 to 1.1 mm; L_e ranges from 2 to 4 mm; and L_L ranges from 6.2 to 7.5 mm as constraints on the dimensions of the proposed antenna, in which $W_p < W_x$, $L_L < L_{patch}$, $L_{stub} < L_{feed}$, and $L_{patch} < W_Y - L_{feed} - L_c$.
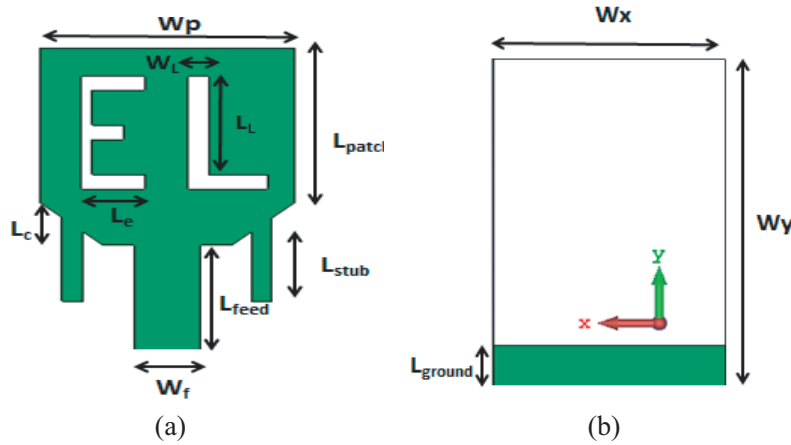

(a)   (b)

Figure 2. The geometry of patch antenna, (a) front side, (b) back side.

W_p is the antenna's width, L_{patch} the antenna's length, h the FR-4 substrate's height, ε_{eff} the effective permittivity, c the speed of light $(3 * 10^8$ m/s), and f_o the center frequency (4.45 GHz). The geometric parameters of the antenna are listed in Table 1. This structure is designed for supporting the following bands: 5G New Radio (NR), sub-6 GHz, and 5 GHz WLAN which covers the frequency range from 3.2 to 5.7 GHz with a center frequency of 4.45 GHz. The dimensions of the printed microstrip patch antenna with partially ground are mounted (at center) above a ground plane with dimensions of 15 mm (in the x-direction) and 23 mm (in the y-direction). There is a fabricated photo of the antenna in Fig. 3. The equivalent circuit of the rectangular patch antenna is shown in Fig. 4.

Table 1. Optimized parameters of the antenna using PSO in (Millimeters).

L_{patch}	11	W_p	12	L_{stub}	6	L_L	7
L_c	2	L_e	3	L_{feed}	6.6	W_f	3.2
W_L	1	W_x	15	W_Y	23	L_{ground}	3

(a)   (b)

Figure 3. Fabrication of antenna, (a) front side, (b) back side.
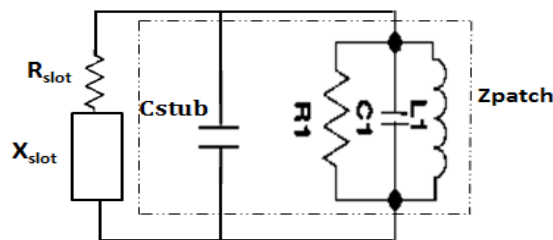
Figure 4. Equivalent circuit of the proposed antenna.

The patch antenna is represented as a parallel combination of resistance R_1, capacitance C_1, and inductance L_1. The values C_1, R_1, and L_1 are calculated using Equations (7), (8), (9), and (10) where R_1 is $50\,\Omega$; L is the total length of the patch; and ω_o is the angular center frequency [34].

$$C_1 = \frac{2W_f\varepsilon_r}{L_h\omega_o^2} \tag{7}$$

$$L_1 = \frac{1}{C_1\omega_o^2} \tag{8}$$

$$C_{stub} = \frac{\varepsilon_o\varepsilon_r L_{stub} * W_{stub}}{h} \tag{9}$$

So the impedance of the rectangular patch antenna can be written as

$$Z_{patch} = \frac{1}{\left(\dfrac{1}{R_1}\right) + \left(\dfrac{1}{j\omega L_1}\right) + (j\omega C_t)}, \tag{10}$$

where $C_t = C_1 + C_{stub}$. The EL slots can be represented as R_{slot} and X_{slot} as shown in Fig. 4. Due to the change in the electrical size of the antenna that results from the slots, the resonance frequency

will change, and the current will flow around EL slots. The currents densely flow in various directions, and the bandwidth will increase due to the merging of these currents. The impedance of the proposed antenna can be calculated from Eq. (11).

$$Z_{in} = \frac{Z_{patch} * Z_{slot}}{Z_{patch} + Z_{slot}}, \quad Z_{slot} = R_{slot} + X_{slot} \tag{11}$$

In this paper, particle swarm is used to get the dimensions of the antenna in addition to the length of stub and dimensions of EL slot to arrive at the objective of a bandwidth ranging from 3.2 to 5.7 GHz to serve the new radio sub-6 GHz.

4. RESULTS AND DISCUSSION

The proposed antenna is simulated using the commercial CST 2019 and fabricated using the photolithographic process as shown in Fig. 3. The antenna is fabricated on a substrate of FR4 material with a dielectric constant of 4.3 and a loss tangent of 0.025. The substrate thickness of the antenna is 1.6 mm. The optimization goals are to reach the smallest dimensions of the antenna in the required bandwidth keeping $|S_{11}|$ below -10 dB by inserting boundaries on the dimensions of an antenna as the minimum and maximum values of the produced antenna's dimensions are defined. The center frequency of the antenna depends mainly on its length as shown in Fig. 5. As the length of the patch increases, the band is shifted to the left side. The bandwidth of the antenna is controlled by the width of the patch as illustrated in Fig. 6. Two parallel stubs are added as another controlling parameter on the bandwidth as shown in Fig. 7 as the bandwidth is increased by reducing the length of stubs. The corresponding vector current distributions of the proposed single antenna without EL slot, with EL slot, and with stubs are shown in Fig. 8 at frequency of 4.5 GHz. It is visualized that the currents are flowing in only one direction as shown in Figs. 8(a), (b), whereas in Figs. 8(c), (d), the currents are densely populated and flowing in various directions. In Fig. 8(c), the currents are populated and flowing in various directions but not as in Fig. 8(d). The currents in Fig. 8(d) are more densely populated. Therefore, the merging of these currents will result in widening the bandwidth, so the bandwidth in Fig. 8(d) is greater than others. Fig. 9 shows the effect of EL slots and effect of stubs on the bandwidth of the antenna. The gain ranges from 3 to 4 dBi while efficiency fluctuates around 90%, as plotted in Figs. 10 and 11, respectively.
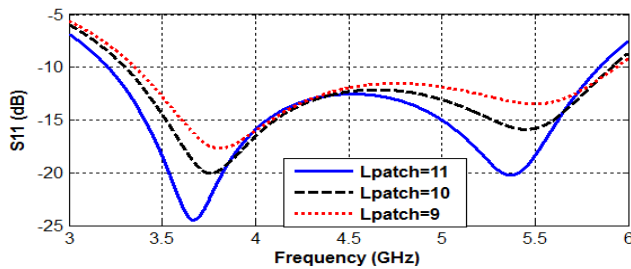

Figure 5. Simulated reflection coefficient for an antenna with several values of L_{patch}.
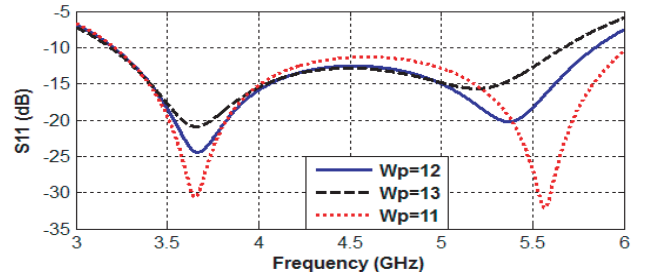

Figure 6. Simulated reflection coefficient for microstrip patch antenna with several values of W_p.

Figure 12 presents the simulated and measured reflection coefficients. The used inertia weight equals 1. When inertia weight is changed to be 0.5, the bandwidth increases but on the expense of a tangential return loss to -10 dB, and this will not be guaranteed in fabrication in addition to increase of the dimensions of the antenna as shown in Fig. 13. The measured results of $|S_{11}|$ show that the antenna can provide -10 dB to -25 dB within the required bandwidth. The antenna can provide bandwidth from 3.2 to 5.7 GHz. The impedance bandwidths obtained are wide enough to cover the bands of 5G New Radio (NR) sub-6 GHz and 5 GHz WLAN. Using the PSO algorithm helps us get the smallest dimensions of the antenna not to increase the cost of fabrication resulting from higher dimensions in
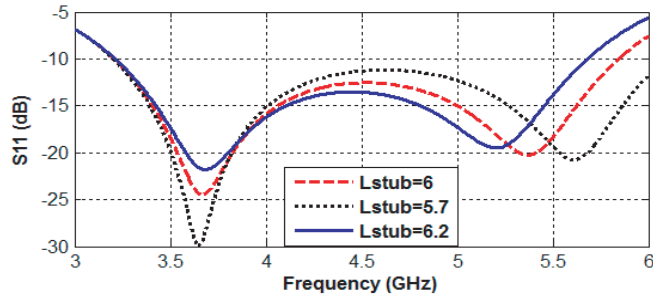
Figure 7. Simulated reflection coefficient for microstrip patch antenna with several values of L_{stub}.
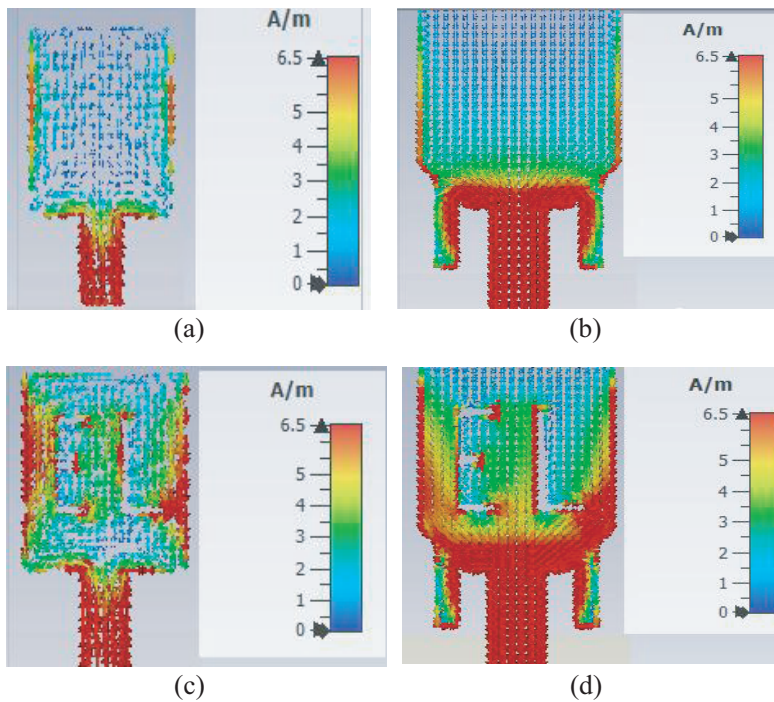

(a)

(b)

(c)

(d)

Figure 8. Vector current density of reference antenna at frequency = 4.5 GHz, (a) with stubs and without EL slot, (b) with EL slot and stubs, (c) with EL slot and without stubs, (d) without slot and without stubs.
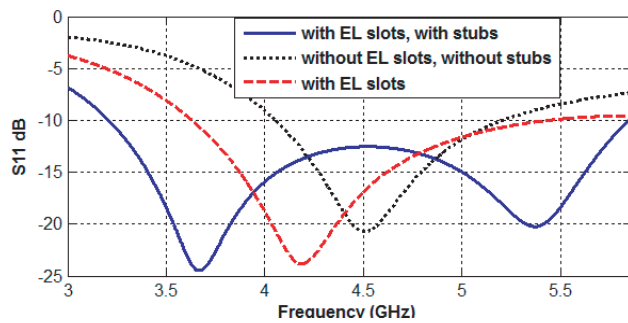

Figure 9. Simulated reflection coefficient for a single antenna without EL slots or stubs, with EL slots, and with EL slots and stubs.
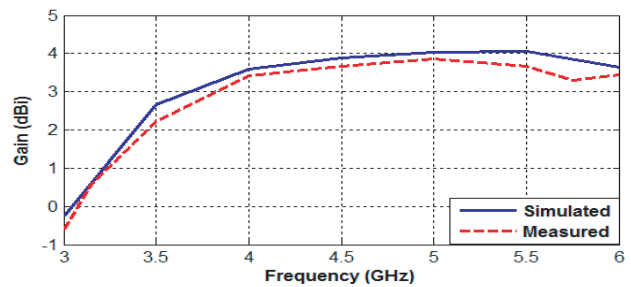

Figure 10. Simulation and Measurement of maximum gain over frequencies for the antenna.
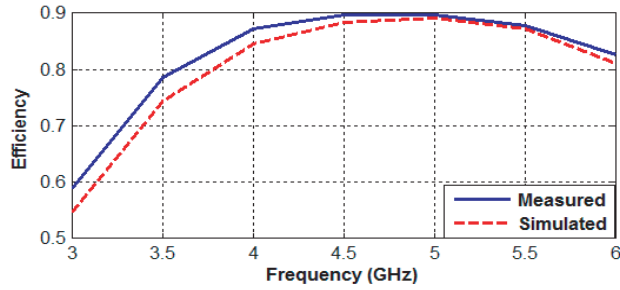
Figure 11. Simulation and Measurement of total efficiency over frequencies for the antenna.
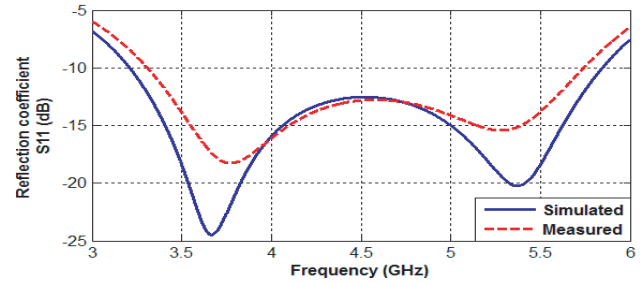

Figure 12. Simulated and measured the reflection coefficient of the antenna.
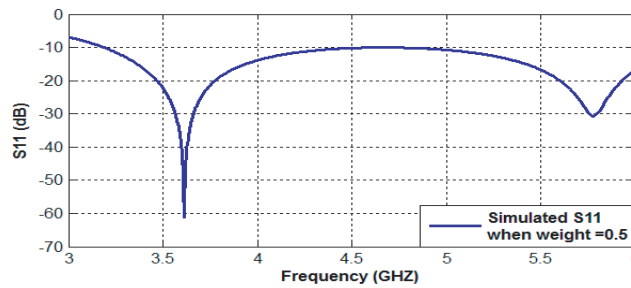

Figure 13. Simulated reflection coefficient of the antenna at inertia weight $= 0.5$.

the required bandwidth. It took less time to give the final dimensions of the antenna as it is faster than designing the antenna depending on trials to achieve the required bandwidth with high gain and high efficiency.

The measured results of radiation pattern at 3.5, 4.5, and 5 GHz are compared with the simulated ones in Fig. 14, and good agreement is obtained. Due to fabrication defects and determining cable losses, there are some discrepancies between simulated and measured results and also due to soldering the SMA connector, but they are still within an acceptable level. The radiation pattern in the elevation plane takes the figure of eight shape at all the operating frequencies and takes the shape of a circle as an isotropic source in the other plane as shown in Fig. 14(d). The results of the radiation pattern parameters of the antenna are shown in Table 2.

Table 2. Results of the radiation pattern of the antenna.

Frequency (GHz)	Parameters at $\Theta = 90^{\mathrm{o}}$ plane		Parameters at $\Phi = 90^{\mathrm{o}}$ plane	
	HPBW	MLM	HPBW	MLM
3.5	88.8^{o}	1.76 dBi	89.4^{o}	2.73 dBi
4.5	85.8^{o}	1.65 dBi	84.5^{o}	2.77 dBi
5	83.1^{o}	1.68 dB	81°	2.86 dBi

The radiation pattern was measured in the Science and Technology Center of Excellence, Egypt, using a compact multiprobe antenna test station (STARLAB-18), VNA model: Agilent E8363B (10 MHz–40 GHz).
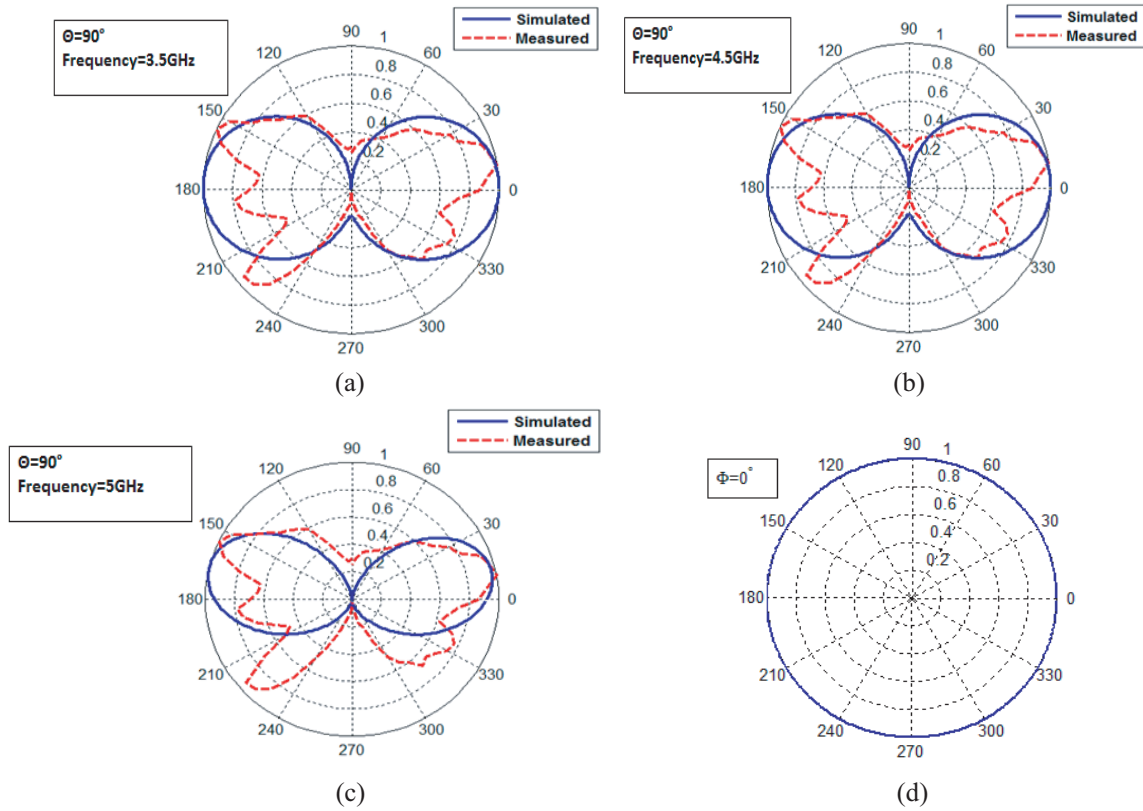
Figure 14. Measured and Simulated radiation pattern at Theta $= 90°$, (a) $f = 3.5\,\text{GHz}$, (b) $f = 4.5\,\text{GHz}$, (c) $f = 5\,\text{GHz}$, (d) Phi $= 0°$.

Table 3. Performance comparison between the proposed design and previous studies.

Ref	substrate	BW GHz	Size mm^3	Gain dBi	Efficiency %
[18]	Ro4350B $\varepsilon_r = 3.48$	0.7 : 0.96 1.71 : 2.7	152 × 152 × 100	8	88
[19]	FR4	1.6 : 2.7	76 × 42 × 1.5	4 : 5	90
[20]	FR4	4.9	31.8 × 17.58 × 1.6	5.8	Not found
[21]	FR4	2.45	72 × 72 × 1.6	Not found	56
[22]	FR4	1.83 : 2.2	300 × 300 × 74.6	2.5	Not found
[23]	RO4300C	1.71 : 2.17	160 × 160 × 60	8	Not found
[24]	FR4	5.2	24 × 16 × 1.5	4.5	Not found
[25]	FR4	1.795 : 2.95	39 × 47.6 × 1.6	3.4	90
[26]	FR4	3.25 : 5.6	20 × 14 × 1.6	2.2	75
Proposed design	FR4	3.2 : 5.7	23 × 15 × 1.6	4	90

5. CONCLUSIONS

In this paper, Particle Swarm Optimization (PSO) algorithm is used to get the dimensions of the antenna and slots. The optimization goals are to reach the smallest dimensions of the antenna in the required bandwidth keeping S_{11} below -10 dB. A microstrip patch antenna with two stubs and EL slots is investigated. The EL slots and two parallel stubs control the desired bandwidth. A prototype of the antenna element with optimized dimensions that are produced from particle swarm has been simulated using CST STUDIO SUITE ver. 2019. The antenna is fabricated on an FR4 substrate with a dielectric constant of 4.3 which reduces the cost of the antenna. The optimization goals are to reach the smallest dimensions of the antenna in the required bandwidth keeping $|S_{11}|$ below -10 dB by inserting boundaries on the dimensions of an antenna as the minimum and maximum values of the produced antenna's dimensions are defined. The initial dimensions used in PSO are obtained from Equations (4), (5), and (6). The antenna is simple in structure and covers the band from 3.2 to 5.7 GHz to find applications in the bands of 5G New Radio (NR) sub-6 GHz n77/n78/n79 and 5 GHz WLAN. It is found that this topology can directly match a 50 Ω feed. The antenna efficiency and gain approaches are 90% and 4 dBi%, respectively. Table 3 summarizes the characteristics of the proposed antenna compared to previous antennas discussed in the literature.

REFERENCES

1. Fang, D.-G., *Antenna Theory and Microstrip Antennas*, CRC Press, 2017.
2. Jackson, D., "Phased array antenna handbook [book review]," *IEEE Antennas and Propagation Magazine*, Vol. 60, No. 6, 124–128, 2018.
3. Pandey, A. K., *Practical Microstrip and Printed Antenna Design*, Artech House, 2019.
4. Lau, H., *Practical Antenna Design for Wireless Products*, Artech House, 2019.
5. Elfergani, I., A.-B. Sadiq, H. J. Rodriguez, and R. Abd-Alhameed, *Antenna Fundamentals for Legacy Mobile Applications and Beyond*, Springer International Publishing, New York, NY, USA, 2018.
6. Mailloux, R. J., *Phased Array Antenna Handbook*, Artech House, 2017.
7. Malik, P. K., S. Padmanaban, and J. B. Holm-Nielsen, eds., *Microstrip Antenna Design for Wireless Applications*, CRC Press, 2021.
8. Ali, E. B., S. S. Kishk, and E. H. Abdelhay, "Multidimensional auction for task allocation using computation offloading in fifth-generation networks," *Future Generation Computer Systems (FGCS)*, Vol. 108, 717–725, Jul. 2020.
9. Gireesha Obaiahnahatti, B., "A literature survey on artificial swarm intelligence-based optimization techniques," *International Journal of Engineering & Technology*, Vol. 7, No. 4.5, 455–458, 2018.
10. Gireesha Obaiahnahatti, B., "A comparative performance evaluation of swarm intelligence techniques," *Journal of Computational Information Systems*, Vol. 14, No. 4, 14–20, 2018.
11. Gireesha, B. and L. Ali, "MATLAB/simulink based design and simulation of square patch microstrip antenna," *Journal of Computational Information Systems*, Vol. 15, No. 1, 143–149, 2019.
12. Jin, N. and Y. Rahmat-Samii, "Advances in particle swarm optimization for antenna designs: Real-number, binary, single-objective and multi objective implementations," *IEEE Transactions on Antennas and Propagation*, Vol. 55, No. 3, 556–567, 2007.
13. Fernaindez Pantoja, M., A. Rubio Bretones, F. Garcia Ruiz, S. G. Garcia, and R. Gomez Martin, "Particle-swarm optimization in antenna design: Optimization of log-periodic dipole arrays," *IEEE Antennas and Propagation Magazine*, Vol. 49, No. 4, 34–47, 2007.
14. Bayraktar, Z., P. L. Werner, and D. H. Werner, "The design of miniature three-element stochastic Yagi-Uda arrays in particle swarm optimization," *IEEE Antennas and Wireless Propagation Letters*, Vol. 5, 22–26, 2006.
15. Tripath, P. K., S. Bandyopadhyay, and S. K. Pal, "Adaptive multi objective particle swarm optimization algorithm," *IEEE Congress on Evolutionary Computation*, 2281–2288, 2007.

16. Merad, L., F. T. Bendimerad, M. S. Mohammed, and S. A. Djennas, "Neural networks for synthesis and optimization of antenna arrays," *Radioengineering-Prague*, Vol. 16, No. 1, Apr. 2007.

17. Megahed, A. A., M. Abdelazim, E. H. Abdelhay, and H. Y. M. Soliman, "Sub-6 GHz highly isolated wideband MIMO antenna arrays," *IEEE Access*, Vol. 10, 19875–19889, Feb. 2022, ISSN: 21693536, DOI: https://doi.org/10.1109/ACCESS.2022.3150278.

18. Huang, H., Y. Liu, and S. Gong, "A dual-patch polarization rotation reflective surface and its application to ultra-wideband RCS reduction," *IEEE Transactions on Antennas and Propagation*, Vol. 16, No. 4, 1111–1114, 2017.

19. Abdullah, H. H., A. A. Megahed, and M.-E. A. Abo-Elsoud, "Low capacity wide-band mobile base station antenna," *IET Microwaves, Antennas & Propagation*, Vol. 13, No. 9, 1345–1349, 2019.

20. Lamsalli, M., A. El Hamichi, and M. Boussouis, "Genetic algorithm optimization for microstrip patch antenna miniaturization," *Progress In Electromagnetics Research Letters*, Vol. 60, 113–120, 2016.

21. Gireesha Obaiahnahatti, B. and L. Ali, "MATLAB/simulink and CST software-based efficiency improved square patch microstrip antenna with PSO algorithm," *Journal of Advanced Research in Dynamical & Control Systems*, Vol. 11, No. 6, 420–428, 2019.

22. El-Gendy, M. S., H. H. Abdullah, and E. A. Abdallah, "Mobile base station dual band microstrip antenna," *IEEE Antennas and Propagation Symp. (AP-S)*, 1839–1840, Memphis, TN, USA, Jul. 2014.

23. Elsherbini, A., J. Wu, and K. Sarabandi, "Dual polarized wideband directional coupled sectorial loop antennas for radar and mobile base-station applications," *IEEE Transactions on Antennas and Propagation*, Vol. 63, No. 4, 1505–1513, Apr. 2015.

24. Kaur, P., "Design of compact and broad-bandwidth rectangular patch antenna using cylindrical rods artificial dielectric," *International Journal of Information Technology*, 1–10, 2021.

25. Verma, R. K. and D. K. Srivastava, "Optimization and parametric analysis of slotted microstrip antenna using particle swarm optimization and curve fitting," *International Journal of Circuit Theory and Applications*, Vol. 49, No. 7, 1868–1883, 2021.

26. Kulkarni, J., A. Desai, and C.-Y. D. Sim, "Wideband four-port MIMO antenna array with high isolation for future wireless systems," *AEU-International Journal of Electronics and Communications*, 128, 2021.

27. Kennedy, J. and R. Eberhart, "Particle swarm optimization," *Proceedings of the IEEE International Conference on Neural Networks*, 1942–1948, 1995, doi: 10.1109/ICNN.1995.488968.

28. Orazio, L. D., "Study and development of novel techniques for PHY layer optimization of smart terminals in the context of next generation mobile communications," University of Trento, Trento, Italy, 2008.

29. Liangfang, N. and D. Sidan, "Evolutionary particle swarm algorithmbased on higher-order cumulant fitting for blind channel identification," *Proceedings of the Wireless Communications, Networking and Mobile Computing*, Oct. 2008.

30. Qiang, W., J. Zhang, and Y. Jing, "Identification of nonlinear communication channel using an novel particle swarm optimization technique," *Proceedings of the International Conference on Computer Science and Software Engineering*, 1162–1165, Dec. 2008.

31. Shami, T. M., A. A. El-Saleh, M. Alswaitti, Q. AL-Tashi, M. A. Summakieh, and S. Mirjalili, "Particle swarm optimization: A comprehensive survey," *IEEE Access on Antennas and Propagation*, Vol. 10, 10031–10061, 2022.

32. Song, C., L. Pan, Y. Jiao, and J. Jia, "A high-performance transmit array antenna with thin metasurface for 5G communication based on PSO (Particle Swarm Optimization)," *Sensors*, Vol. 20, 1–15, 2020.

33. Kang, M. S., Y. J. Won, B. G. Lim, and K. T. Kim, "Efficient synthesis of antenna pattern using improved PSO for space borne SAR performance and imaging in presence of element failure," *IEEE Sensors Journal*, Vol. 18, 6576–6587, 2018.

34. Verm, S. and J. A. Ansari, "Analysis of U-slot loaded truncated corner rectangular microstrip patch antenna for broadband operation," *AEU-International Journal of Electronics and Communications*, Vol. 69, No. 10, 1483–1488, 2015.